



1
2
3
4
5
6
7
8
9
10
11
12
13
14
15
16
17
18
19
20
21
22
23
24
25
26
27
28
29
30
31
32

DR. MARIJN BAUTERS (Orcid ID : 0000-0003-0978-6639)

DR. TRAVIS WILLIAM DRAKE (Orcid ID : 0000-0002-7564-974X)

PROF. HANS VERBEECK (Orcid ID : 0000-0003-1490-0168)

Article type : Primary Research Articles

Century-long apparent decrease in iWUE with no evidence of progressive nutrient limitation in African tropical forests

Running title: A century of change in the Congo Basin forest

Marijn Bauters^{1,2,†}, Sofie Meeus^{3,†}, Matti Barthel⁴, Piet Stoffelen³, Hannes P.T. De Deurwaerder², Félicien Meunier², Travis W. Drake⁴, Quentin Ponette⁵, Jérôme Ebuy^{5,6}, Pieter Vermeir⁷, Hans Beeckman⁸, Francis wyffels⁹, Samuel Bodé¹, Hans Verbeeck², Filip Vandeloock³, Pascal Boeckx¹

¹ Isotope Bioscience Laboratory – ISOFYS, Department of Green Chemistry and Technology, Faculty of Bioscience Engineering, Ghent University, Coupure Links 653, 9000 Gent, Belgium

² Computational and Applied Vegetation Ecology – CAVElab, Department of Environment, Faculty of Bioscience Engineering, Ghent University, Coupure Links 653, 9000 Gent, Belgium

³ Meise Botanic Garden, Domein Bouchout, Nieuwelaan 38, 1860 Meise, Belgium

⁴ Sustainable Agroecosystems, Department of Environmental Systems Science, ETH Zürich, Tannenstrasse 1, 8092 Zürich, Switzerland

⁵ UCL-ELI, Earth and Life Institute, Université Catholique de Louvain, Croix du Sud 2, L7.05.09, B-1348 Louvain-la-Neuve, Belgium

⁶ Université de Kisangani (UNIKIS/FGRNR), BP 2012, Kisangani, République Démocratique du Congo

33 ⁷ Laboratory for Chemical Analyses – LCA, Department of Green Chemistry and Technology, Ghent University,
34 Ghent, Belgium

35

36 ⁸ Royal Museum for Central Africa, Tervuren, Belgium

37

38 ⁹ AIRO, Electronics and Information Systems Department, Ghent University-Imec, Ghent, Belgium.

39 † M. Bauters and S. Meeus should be considered joint first author.

40 e-mail: Marijn.Bauters@UGent.be, sofie.meeus@plantentuinmeise.be

41 Phone: +32 9 264 60 06

42 **Abstract**

43 Forests exhibit leaf and ecosystem level responses to environmental changes. Specifically, rising carbon
44 dioxide (CO₂) levels over the past century are expected to have increased the intrinsic water-use
45 efficiency (iWUE) of tropical trees while the ecosystem is gradually pushed into progressive nutrient
46 limitation. Due to the long-term character of these changes, however, observational datasets to validate
47 both paradigms are limited in space and time. In this study, we used a unique herbarium record to go
48 back nearly a century and show that despite the rise in CO₂ concentrations, iWUE has decreased in
49 central African tropical trees in the Congo basin. Although we find evidence that points to leaf-level
50 adaptation to increasing CO₂ – i.e. increasing photosynthesis-related nutrients and decreasing maximum
51 stomatal conductance, a decrease in leaf $\delta^{13}\text{C}$ clearly indicates a decreasing iWUE over time.
52 Additionally, the stoichiometric carbon to nitrogen and nitrogen to phosphorus ratios in the leaves show
53 no sign of progressive nutrient limitation as they have remained constant since 1938, which suggests
54 that nutrients have not increasingly limited productivity in this biome. Altogether, the data suggest that
55 other environmental factors, such as increasing temperature, might have negatively affected net
56 photosynthesis and consequently downregulated the iWUE. Results from this study reveal that the
57 second largest tropical forest on Earth has responded differently to recent environmental changes than
58 expected, highlighting the need for further on-ground monitoring in the Congo Basin.

59
60 **Keywords:** Congo basin, CO₂ fertilization, herbarium, photosynthesis, stomata, aggravated nutrient
61 limitation, tropical forest, water use efficiency

62 Introduction

63 The Earth system has been subjected to unprecedented changes over the past century, including
64 increasing atmospheric carbon dioxide (CO₂) levels, shifting rainfall regimes, and changes in global
65 biogeochemical cycles (Steffen et al. 2015). Uncertainties in the future response of forest ecosystems to
66 these environmental changes are perhaps most prominent in the tropics, where monitoring is
67 underdeveloped compared to temperate regions (Schimel et al. 2015). Tropical forests comprise 55% of
68 the current carbon (C) stock of the world's forests and exhibit high gross (GPP) and net (NPP) primary
69 productivity (Beer et al. 2010, Pan et al. 2011). As such, tropical forests play a pivotal role in the global C
70 cycle. The effect of human-induced changes on this biome is thus a central question in global change
71 research (Bonan 2008a, Gibson et al. 2011). Large-scale permanent monitoring plots and tree-ring
72 research in tropical forests have shown varying trends in tree growth over the last decades, from
73 increased (Phillips 1998, Baker et al. 2004, Lewis et al. 2009) to stable or decreased growth (Feeley et al.
74 2007, Clark et al. 2010, Groenendijk et al. 2015, Van Der Sleen et al. 2015). One of the proposed drivers
75 for a growth acceleration is the global increase in atmospheric CO₂ concentration, i.e. CO₂ fertilization,
76 which supposedly increases the intrinsic water-use efficiency (iWUE) – i.e. the ratio of C gain to water
77 loss- or photosynthetic rates of terrestrial plants (Ballantyne et al. 2012, Keenan et al. 2013, Lavergne et
78 al. 2019). Indeed, increases of iWUE have been widely noted across the tropics (Hietz et al. 2005, Brien
79 et al. 2010, Nock et al. 2011, Van Der Sleen et al. 2015), but few studies have disentangled whether this
80 iWUE adaptation is controlled by shifts in photosynthesis (A) or stomatal conductance (g_s) (Bonal et al.
81 2011).

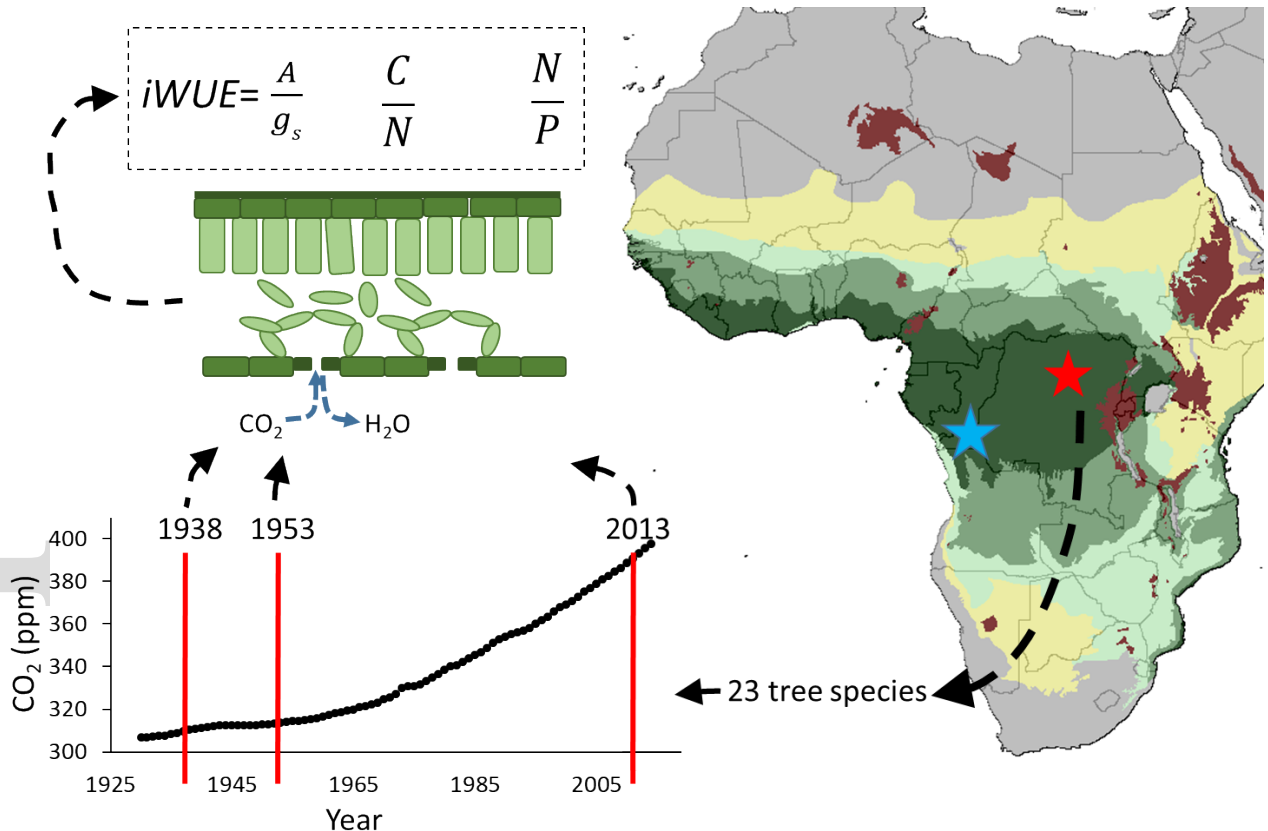
82
83 Consequently, the question arises whether nitrogen (N) and phosphorus (P) supply can meet the
84 increased biomass accrual from CO₂ fertilization of forests globally. Modeling efforts have initially
85 predicted a dampening of the land C storage sensitivity to CO₂ caused by N limitation (Bonan 2008b,
86 Sokolov et al. 2008). More recent simulations predict a reduction of 25% of the projected NPP by 2100 if
87 both N and P limitations are taken into account (Wieder et al. 2015). To date, the empirical evidence of
88 this progressive nutrient limitation remains inconclusive. A limited number of studies showed that long-
89 term N effects are regionally distinct, including decreasing N availability in North American grasslands
90 and forests (McLauchlan et al. 2010, 2017) and European forests (Jonard et al. 2015), but increasing N
91 availability in Panama and Thailand (Hietz et al. 2011). Moreover, recent evidence suggests a general
92 decrease in N supply relative to the N demand in natural ecosystems worldwide (Craine et al. 2018). At
93 present, the long-term effects of changes in N availability within these biomes remain poorly
94 understood. Additionally, despite the fact that P is considered the major limiting nutrient for tropical
95 forest ecosystems, only a few studies have looked directly into progressive P limitation (Vitousek et al.
96 2010). Theory predicts that an initial P limitation might be exacerbated under CO₂ fertilization and/or

97 elevated reactive atmospheric N deposition because litter stoichiometry will become increasingly
98 depleted in P, which results in lower net P mineralization rates and finally further P limitation to plant
99 growth (Peñuelas et al. 2013, Fernandez-Martinez et al. 2014, Wieder et al. 2015, Fleischer et al. 2019).
100 Evidence from primary succession and nutrient addition experiments shows that progressive P limitation
101 results in a shift in leaf P content and the N:P ratio in the canopy (Izquierdo et al. 2013, Li et al. 2016),
102 while progressive P limitation over time has only been observed in a few sites (Huang et al. 2016).

103
104 Most knowledge that we have gained on ecosystem responses to environmental change comes from
105 short-term experiments or modeling studies. While these studies increase our process-based
106 understanding of separate global change drivers, long-term empirical data are required to verify many of
107 the paradigms that have been put forth. Indeed, empirical datasets are constrained by experiment
108 duration, funding timelines, and the historic absence of researchers in many tropical sites. However,
109 historical herbarium records can overcome some of these experimental limitations and enable us to go
110 back in time to validate the overall response of tree species (Meineke et al. 2018). The UNESCO
111 Yangambi Man and Biosphere Reserve, in the heart of the Congo basin, holds a research center founded
112 in the 1930s by the colonial Belgians and passed on to a Congolese research institute in 1962. The
113 continuous presence of researchers since 1930 has led to one of the most extensive and oldest
114 herbarium collections in central Africa. From that collection, we selected 23 tree species common to
115 central African tropical forests that cover a range of ecological life-history traits. We used herbarium
116 specimens from three different time periods to accomplish three goals: 1) quantify responses in $iWUE$
117 from 1938 until present, 2) determine whether this response is caused by changes in g_s or
118 photosynthesis, or a combination of both, and 3) provide evidence of increasing nutrient limitation, i.e.
119 to assess whether the relative N and P demand kept pace with the induced changes on an ecosystem
120 level. These goals were accomplished through the measurement of foliar nutrient content, isotopic
121 signatures, and stomatal traits. Furthermore, we used an additional extensive sample set, along with a
122 modelling effort, to rule out potential sampling biases in the effects that we quantified on the herbarium
123 specimens.

124
125 **Methods**
126 **Historic sample set.** We used herbarium specimens of 23 tropical tree species that are common to
127 central Africa, belonging to 14 flowering plant families (Table S1) and originating from the same reserve
128 in the Democratic Republic of Congo. Leaves were collected from the African herbarium collection of
129 Meise Botanic Garden, Belgium. The herbarium specimens were all collected in the Yangambi Man and
130 Biosphere Reserve (N 00°47'; E24°30'), situated on the Northern bank Congo River 100 km west of
131 Kisangani. The region has an Af-type tropical rainforest climate, with an annual rainfall of 1750 mm, a

132 bimodal rainfall distribution exhibiting a longer and shorter dry season, and a stable temperature of
 133 24.5°C throughout the year. The site is dominated by ferralsols (Van Ranst et al. 2010). Material was
 134 sampled from specimens collected at three different time points: (1) 1935-1938 (hereafter 1938), (2)
 135 1951-1953 (hereafter 1953), (3) 2012-2013 (hereafter 2013). For most species, we sub-sampled three
 136 specimens per time period, resulting in nine specimens per species (Table S1). We specifically targeted
 137 samples from the same reserve for the entire sample set, to eliminate inter-site variability or local
 138 climate effects. Additionally, the three dates were specifically selected to maximize the time range:
 139 sample collection started in the Democratic Republic of Congo around 1935 and stopped momentarily
 140 after the independence in 1960. To our knowledge, the historic samples were taken from sunlit,
 141 flowering or fruiting branches from adult trees (pers. comm., Piet Stoffelen). The samples in 2013 were
 142 collected with tree climbers, which implies that this sample set comprises both sun and shade leaves,
 143 because of the practical difficulties of access in the upper canopy. In all cases, only fully expanded, adult
 144 leaves were sampled.



145
 146 **Figure 1.** The location of Yangambi (red star), where triplicate samples were taken from 23 different tree
 147 species around the years 1938, 1953 and in 2013. The samples were all analyzed to detect changes over
 148 time via proxy variables for photosynthesis (A), stomatal conductance (g_s), intrinsic water-use efficiency
 149 (iWUE) and leaf stoichiometric carbon to nitrogen (C:N) and nitrogen to phosphorus (N:P) ratios. The
 150 coloration on the map shows the ecosystem type delineation, with tropical wet forest in dark green. The

151 blue star indicates the location of the Luki reserve, where some of the samples to quantify variability in
152 stomatal traits were taken.

153
154 **Stoichiometry and isotopic composition.** For each herbarium specimen, one leaf was sampled in the
155 least invasive way possible by punching a hole with a hole-puncher in the center of the leaf on the right
156 side of the central vein (upper side of the leaf pointing upwards). Leaf C, N and $\delta^{13}\text{C}$ of plant samples
157 were analyzed using an elemental analyzer (Automated Nitrogen Carbon Analyser; ANCA-SL, SerCon,
158 UK), interfaced with an Isotope Ratios Mass Spectrometer (IRMS; 20-22, SerCon, UK). To check if the bulk
159 $\delta^{13}\text{C}$ signal was consistent with the cellulose $\delta^{13}\text{C}$ signal, we analyzed cellulose $\delta^{13}\text{C}$ for a subset of the
160 samples (n=27). For this, we used an α -cellulose extraction protocol, modified for speed and small
161 sample extraction (Brendel et al. 2000, Evans and Schrag 2004). In short, we weighed ca. 2 mg of bulk
162 leaf material into 1.5 mL screw-cap polyethylene tubes and added 240 μl 80% acetic acid and 24 μl 69%
163 nitric acid. The tubes were capped and placed in a 120°C oil bath for 30 minutes. After cooling of the
164 samples to room temperature, 800 μl 100% ethanol was added to the tubes, and the tubes were
165 centrifuged for 5 minutes at 15500 g. Next, three sequential rinse steps were performed by adding 1)
166 600 μl deionized water, 2) 300 μl 100% ethanol and 3) 500 μl acetone with the centrifugation step
167 between each rinse to remove the supernatant. Finally, the tubes were dried in an oven for 30 minutes
168 at 50°C. The $\delta^{13}\text{C}$ signal of the extracted cellulose was analyzed as described for the bulk leaf material
169 above. We sampled the same leaves a second time with a hole puncher and analyzed the bulk material
170 for the for the leaf $\delta^{18}\text{O}$ values using a high temperature Thermal Conversion Elemental Analyzer (TC-EA),
171 interfaced with an IRMS (IRMS; 20-20, SerCon, UK). In addition to C and O isotope analysis, between 0.2
172 and 0.5 g of leaf sample was dry-ashed at 550°C for 5.5 hours; the ash was dissolved in 2M HCl solution
173 and subsequently filtered through a P-free filter. The aliquots were then analyzed for P and Mg by
174 inductively-coupled plasma atomic emission spectroscopy (ICP AES, IRIS interpid II XSP, Thermo scientific,
175 USA; Ryan *et al.* 2001). Stoichiometric C:N, N:P and C:P ratios that were calculated are all mass ratios.

176
177 **Stomatal traits.** Leaf impressions were made from the abaxial side of five leaves per specimen halfway
178 between the main vein and margin of the leaf, equidistant from the tip and base of the leaf blade.
179 Transparent varnish was used to make the impressions, which were mounted with double-sided tape on
180 a microscope slide after drying. Three photomicrographs of 1600x1200 pixels were taken per leaf print
181 (dimensions = 344x258 μm ; area view field = 0.09 mm^2) using a digital stacking microscope (VH-5000 Ver
182 1.5.1.1, KEYENCE CORPORATION, Osaka, Japan) with full coaxial lightning and default factory settings for
183 shutter speed at $\times 1000$ lens magnification (VH-Z250R). In order to determine the stomatal density of our
184 dataset, we first trained a stomata detector model. Briefly, we started from the deep learning approach
185 discussed in Meeus *et al.* (under review), which comprises a patch-based approach and starts from the

186 pre-trained convolutional layers of the VGG19 architecture (Simonyan and Zisserman 2014) by using the
187 imagenet dataset (Deng et al. 2009). The output of the convolutional layers is then fed into a classifier
188 network consisting of two dense layers, with 4096 and 2048 neurons, respectively and one output
189 neuron. The weights of the classifier network were trained using the Adam learning rule (Kingma and Ba
190 2015) with batch size 128. The training set consisted of 8,500 positive and 48,500 negative patches,
191 which were sampled from the 18 species for which leaf prints and high-quality microphotographs were
192 available. In order to avoid over-fitting, the weights of the dense layers were trained using dropout.
193 Furthermore, data augmentation was used to enrich the training set by flipping and rotating the patches
194 as well by varying the contrast, brightness, and sharpness. The model described in Meeus et al. (under
195 review) was adjusted to increase accuracy of stomatal detection by optimizing the threshold for each of
196 the species separately on a validation set consisting of three microphotographs per species. Threshold
197 and information retrieval standard measures such as precision, recall and F-score to evaluate the
198 model's performance are shown in Table S2. Stomatal counts were converted to stomata per square
199 millimeter. Guard cell length was manually measured in one stoma per picture on a subset of on average
200 10 pictures per herbarium specimen using Fiji (Schindelin et al. 2012).

201
202 **Variance sample set.** To gain insight in how variance is structured within crown, individual, and species,
203 we performed a decomposition of intra-specific variance for a subset of the studied species. For the leaf
204 chemical and isotope composition, we looked at intra-species variability for two species:
205 *Gilbertiodendron dewevrei* (four trees) and *Mammea africana* (two trees) sampled in 2012, in the same
206 reserve as where the herbarium samples were taken. From each individual tree, triplicate leaf samples
207 were collected at three canopy heights (low, middle, and upper) during six different sampling events.
208 For this sample set, we used whole ground leaves, which were analyzed the same way as the time series
209 sample set. For the stomatal traits, we used samples of four species: *Prioria balsamifera* (four
210 individuals), *Prioria oxyphylla* (two individuals), *Polyalthia suaveolens* (three individuals), *Trichilia*
211 *gilgiana* (three individuals). For each individual, 3 specimens were collected: one at the base of the
212 crown, one in the middle, and one at the top. The latter samples were collected in the Luki reserve at a
213 different location in the Democratic Republic of Congo, Eastern DRC, in 2016 (Figure 1).

214
215 **Data analyses.** For the calculation of the iWUE we derived historic $\delta^{13}\text{C-CO}_2$ ($\delta^{13}\text{C}_a$) values from the
216 equation in Bonal et al. (2011), which are in turn based on earlier work by Keeling et al. (1989) and Friedli
217 et al. (1986), correcting for the Suess effect. For historic atmospheric CO_2 concentrations (C_a), we fitted a
218 second-order polynomial regression to monitoring data from Mauna Loa and extrapolated back to 1935
219 and 1953 (dataset available at <ftp://aftp.cmdl.noaa.gov/>). We used the classic model of C isotope

220 discrimination during photosynthesis to derive leaf $\Delta^{13}\text{C}$ from these data and the cellulose $\delta^{13}\text{C}$, which
221 were obtained via the bulk leaf $\delta^{13}\text{C}$ measurements (Figure S2, Farquhar et al. 1982):

$$\Delta^{13}\text{C}_{cell} = \frac{\delta^{13}\text{C}_a - \delta^{13}\text{C}_{cell}}{1 + \delta^{13}\text{C}_{cell}} \quad (1)$$

222 Likewise, if we do not take into account respiration-related fractionation, we know that carbon isotope
223 discrimination can be described by:

$$\Delta^{13}\text{C}_{cell} = a + (b - a)\frac{C_i}{C_a} - \frac{f\Gamma^*}{C_a} \quad (2)$$

224 where the first term is the fractionation during CO_2 diffusion through the stomata ($a=4.4\%$; O'Leary,
225 1981), the second term the fractionation associated with reactions by Rubisco and PEP carboxylase
226 ($b=27\%$; Farquhar and Richards 1984), and the third term fractionation through photorespiration
227 ($f=12\%$ with Γ^* the CO_2 compensation point in the absence of day respiration ≈ 40 ppmv; Farquhar et al.
228 1982, Keeling et al. 2017, Schubert and Jahren 2018, Lavergne et al. 2020). Hence, the CO_2 concentration
229 in the stomatal cavity (C_i) can therefore be calculated as follows:

$$C_i = \frac{C_a(\Delta^{13}\text{C}_{cell} - a) + f\Gamma^*}{b - a} \quad (3)$$

230 Furthermore, we know that iWUE is related to the ratio of photosynthesis (A) to stomatal conductance
231 (g_s), and given by:

$$\text{WUE} = \frac{A}{g_s} = \frac{C_a}{1.6} \left(1 - \frac{C_i}{C_a}\right) \quad (4)$$

232 For the trends of all chemical or stomatal traits over time, we fitted linear mixed effects models with
233 species as a random effect and the sampling period as a categorical fixed effect. Models were then fitted
234 using maximum likelihood methods in the 'lme4' package in R (Bates et al. 2007). P-values for fixed
235 effects were determined based on the denominator degrees of freedom calculated with the
236 Satterthwaite approximation, in the 'lmerTest' package (Kuznetsova et al. 2014). Given the distinctness
237 of legumes in plant physiology (Adams et al. 2016), we repeated the analysis while adding a two-level
238 factorial fixed effect to separate *Fabaceae* and non-*Fabaceae* trees as potential N fixers, allowing for the
239 interaction between sampling data and this new grouping variable.

240
241 For the decomposition of intraspecific variance in leaf chemistry and stomatal traits into inter-individual
242 and intra-crown variance, we first fitted a random effects model with nested random effects, i.e. crown
243 level nested in individual, and with species as a fixed effect. We subsequently extracted the variance that
244 was estimated to be associated with the different nesting levels and considered it to be the 'structural

245 variation' with the respective level. Second, we re-fitted a mixed effect model for all response variables,
246 but now with the crown position (upper canopy, middle, and lower canopy) as an additional fixed effect
247 with species, instead of a random effect nested in individual. This was done to explicitly estimate the
248 effects of sampling height in the canopy, on the different response parameters. For this decomposition
249 of variance, we used the Bayesian multilevel model package 'brms' (Bürkner 2017), with weakly
250 informed Gaussian prior distributions for all effects. After fitting, the estimates of variance were
251 extracted via the posterior distributions of the random error terms, and additionally also via the
252 posterior distributions of the factor levels for the fixed effects for the second model fits including crown
253 position as a fixed effect. For all statistical analysis, R was used (R Development Core Team 2018).

254
255 **Sensitivity of $\delta^{18}\text{O}$ to changes in g_s .** Earlier work has pointed out the limited sensitivity of $\delta^{18}\text{O}$ in
256 conditions of high relative humidity (Farquhar et al. 2007, Roden and Siegwolf 2012). To quantify the
257 sensitivity of $\delta^{18}\text{O}$ to changes in g_s , we used a recent model from dendrochronology, developed by
258 Barbour et al. (2004), and further improved by Lorrey et al. (2016). For ease of interactive use, we
259 translated the model into a Microsoft Excel tool that simulates changes in leaf $\delta^{18}\text{O}$ as function of
260 stomatal conductivity shifts, relative humidity, temperature, photosynthetic active radiation, and source
261 water and atmospheric water $\delta^{18}\text{O}$ signature (Appendix 1, Figure S1). We parameterized this for our
262 central African site, and assessed potential changes in leaf $\delta^{18}\text{O}$ as a response to changes in g_s , at
263 different levels of relative humidity. For this, we assumed a constant temperature of 25°C, a wind speed
264 of 3.1 m s⁻¹, a photosynthetic active radiation of 1000 $\mu\text{mol m}^{-2} \text{s}^{-1}$, and an effective path length of 0.1 m,
265 which corresponds to recent on-site measurements. Additionally, we used this tool to assess how
266 sensitive a stomatal conductance-induced change in leaf $\delta^{18}\text{O}$ was to changes in temperature, leaf width,
267 effective path length, photosynthetic active radiation, atmospheric pressure, wind speed and source
268 water isotope composition, at high relative humidity (90%).

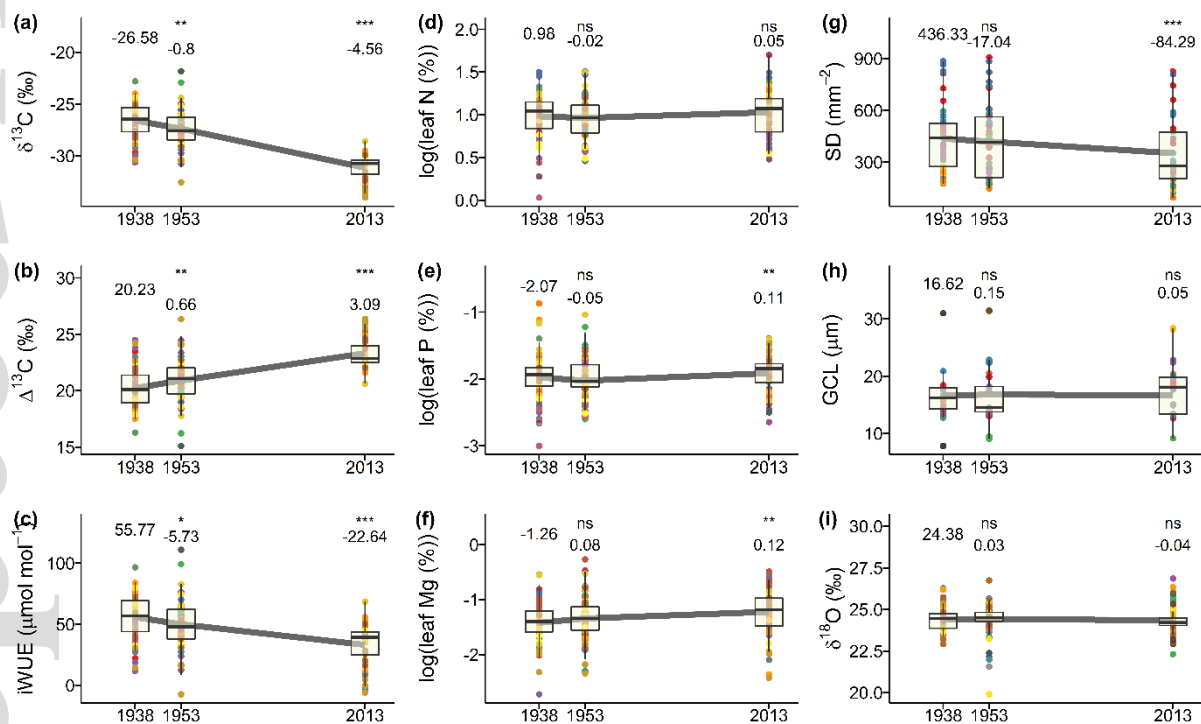
269 270 **Results**

271 **Trends in leaf stable isotope signatures and nutrients.** The sampled species set comprises species with
272 leaf N values ranging from 1.30 to 4.29% and wood density values from 219 to 841 kg m⁻³, including both
273 N fixers and non-N fixers. Overall, leaf $\delta^{13}\text{C}$ decreased from -26.6‰ in 1938 to -31.9‰ in 2013 (Figure
274 2a). This decrease implies an overall increase in $\Delta^{13}\text{C}_{\text{leaf}}$ from 20.2‰ in 1938 to 23.9‰ in 2013 (Figure
275 2b). Consequently, estimated iWUE decreased on average from 55.8 to 27.4 (Figure 2c). The leaf
276 cellulose $\delta^{13}\text{C}$ showed a strong positive correlation with bulk leaf $\delta^{13}\text{C}$ (Figure S2; $R^2=0.75$; P-value <
277 0.001). Leaf P and Mg showed an increase from 1953 to 2013 (Figure 2e and 2f), while leaf N did not
278 change significantly (Figure 2d). Likewise, the leaf $\delta^{18}\text{O}$ signature did not change over time (Figure 2i).

279 The analysis, including the interaction between non- and potential N-fixers, revealed that iWUE
 280 significantly decreased in both non N-fixers and in N-fixers, but faster in non N-fixers (Figure S3c).
 281

282 **Trends in stomatal traits.** Automatic detection of stomata gained accurate stomatal counts except for
 283 one species, *Irvingia grandifolia* with a F-score of only 0.58 (Table S2) which was therefore omitted from
 284 further stomatal analyses. Stomatal densities across species and time ranged from 22 mm⁻²
 285 (*Strombosiopsis tetrandra*) to 1089 mm⁻² (*Entandrophragma candollei*) (Figure S5). Guard cell size ranged
 286 from 6 μm to 37 μm. The stomatal density decreased from an average of 368 to 245 stomata mm⁻², while
 287 the average guard cell length did not change significantly over time. Additionally, the guard cell length
 288 (GCL) increased in N fixers contrary to non-N fixers (Figure S3h). The leaf stoichiometric responses were
 289 not different in potential N fixers versus non-fixers (Figure S4).

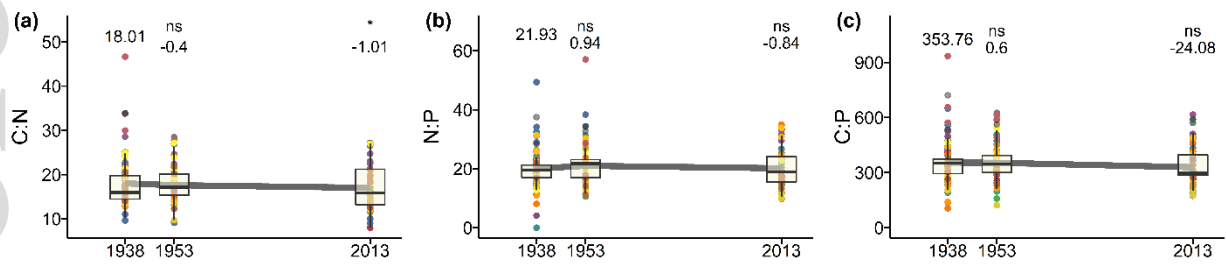
290



291

292 **Figure 2.** Trends of leaf carbon stable isotopic composition (a and b) and intrinsic water-use efficiency
 293 (iWUE, c); leaf nitrogen (N, d), leaf phosphorus (P, e) and leaf magnesium (Mg, f) which are nutrient
 294 proxies related to photosynthesis; and stomatal density (SD, g) and guard cell length (GCL, h) and the
 295 stable oxygen isotopic signature (i) over the last century in central African tropical forest. In all plots the
 296 left value is the baseline value for 1938, followed by the significance of change with the effect estimates
 297 for 1953, and the significance and effect size for 2013 with respect to 1953, with three levels of
 298 significance: $P < 0.001$ (***), $P < 0.05$ (**) and $P < 0.1$ (*). Different colors indicate the 23 different
 299 species that were included in the analyses, with the grey line the overall fixed effect of the fitted models.

300



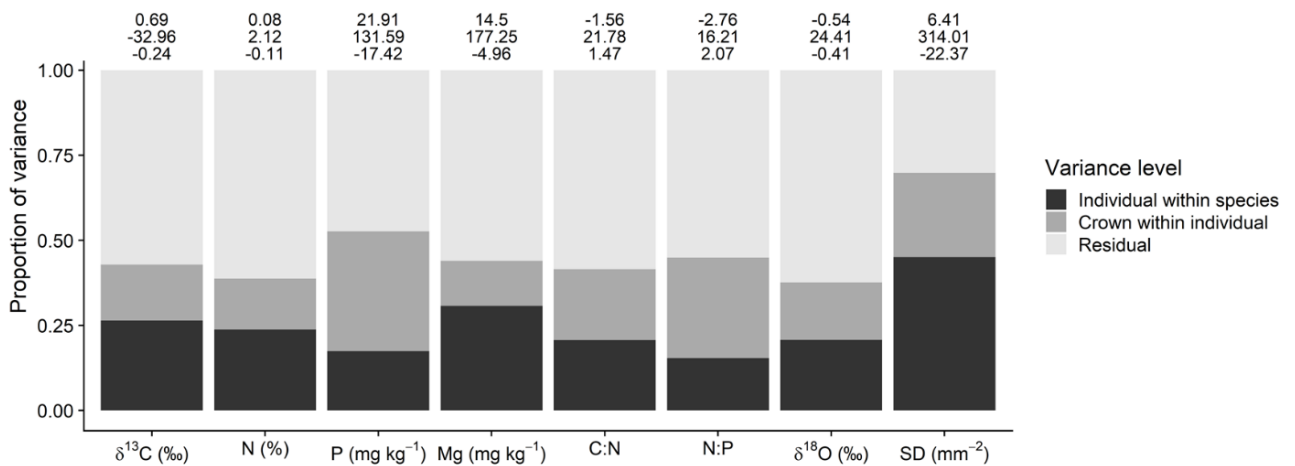
301

302 **Figure 3.** Shifts in foliar C:N (a), N:P (b) and C:P (c) mass ratio stoichiometry since 1938 for central African
 303 trees. In all plots the left value is the baseline value for 1938, followed by the significance of change with
 304 the effect estimates for 1953, and the significance and effect size for 2013 with respect to 1953, with
 305 three levels of significance: $P < 0.001$ (***), $P < 0.05$ (**) and $P < 0.1$ (*). Different colors indicate the 23
 306 different species that were included in the analyses, with the grey line the overall fixed effect of the
 307 fitted models.

308

309 **Variance of isotopes, leaf chemistry and stomatal traits within the canopy.** The structural variance
 310 associated with crown sampling height for leaf N, P, and N:P was higher within an individual than
 311 between individuals of the same species, but lower for all other measured variables (Figure 4). For leaf N
 312 and P, 16% and 35% of the intraspecific variation was associated with the sampling position in the crown,
 313 respectively, resulting in 29% for the leaf N:P stoichiometry. The isotope signatures were much less
 314 sensitive to crown sampling level for leaf $\delta^{13}\text{C}$ and leaf $\delta^{18}\text{O}$ with 17% and 16% of the variation,
 315 respectively. Stomatal density (SD) and leaf magnesium exhibited especially high inter-individual
 316 variability (45% and 32%, respectively) and intra-crown variance (25% and 13%, respectively). The
 317 additional model fits including crown-height as a fixed effect revealed that sun leaves exhibit higher leaf
 318 $\delta^{13}\text{C}$, leaf N, P, and Mg, and stomatal density values than shade leaves, while the inverse was noted for
 319 leaf C:N, N:P, and $\delta^{18}\text{O}$ signatures. The largest relative effects were for leaf P (16% higher in upper
 320 canopy vs. middle canopy), and leaf N:P (-17%), with all other variables exhibiting effects $< 10\%$ (Figure
 321 4).

322



323
324

325 **Figure 4.** Intra-specific variability, decomposed into inter-individual and intra-crown variability of the
 326 measured stable isotope signatures, leaf nutrients and the stomatal density (SD) of the leaves based on
 327 two present-day sample sets from Yangambi and Luki, respectively, in the Democratic Republic of Congo.
 328 The bars indicate the relative variance associated with each of the levels; numbers above the plot give
 329 the specific effect of sampling in the upper or lower canopy (respectively highest and lowest line) versus
 330 the canopy values in the center of the canopy (middle line).

331

332 **Sensitivity of $\delta^{18}\text{O}$ to changes in stomatal conductance.** The simulated leaf $\delta^{18}\text{O}$ value as a function of g_s
 333 clearly shows a decreasing $\delta^{18}\text{O}$ response with increasing relative humidity, all other parameters kept
 334 constant. If we assume a doubling of the stomatal conductivity over time, the resulting shift in leaf $\delta^{18}\text{O}$
 335 value would be 0.6‰, if relative humidity is near 100% (Appendix 1 for additional scenarios, Figure S1).
 336 Additionally, we used the tool to assess the sensitivity of stomatal conductance-induced changes in leaf
 337 $\delta^{18}\text{O}$ to any of the other parameters that are needed for the calculations. Our sensitivity analysis (at a
 338 relative humidity of 90%, and assuming that g_s doubles), shows that increasing any of the parameter
 339 values with 50% does not change the leaf $\Delta^{18}\text{O}$ (i.e. the signal we would have to capture with an IRMS
 340 after a doubling of the g_s over time) with more than 0.3‰ (Appendix A1).

341

342 Discussion

343 **Morphological and chemical leaf adaptation to increasing CO_2 , but decreasing iWUE.** Our study site in
 344 central Africa exhibits a clear decreasing iWUE across the sampled species, and is thereby apparently
 345 paradoxical in its response to environmental change. Indeed, in the wake of CO_2 fertilization, increasing
 346 iWUE has been widely reported from boreal and temperate forests (e.g. Keenan et al. 2013, Wang et al.
 347 2018). There are only few studies for tropical forests (Cernusak et al. 2013) and most studies show either

348 increasing iWUE (Hietz et al. 2005, Silva et al. 2009, Brienen et al. 2010, Nock et al. 2011, van der Sleen et
349 al. 2014) or no significant change (Bonal et al. 2011). The question arises whether our observed decrease
350 in iWUE is driven by decreasing A or increasing g_s . To disentangle this, we looked at stomatal density and
351 guard cell length, which directly signal maximal g_s . The combination of a stable guard cell length, with a
352 decreasing stomatal density, suggests an optimization for reduced water loss on the leaf level. Indeed, it
353 seems that leaves in central African forests are down-regulating stomatal densities as a response to
354 increased CO_2 (Xu et al. 2016) or other factors such as increased vapor pressure deficit (Figure S7, Jiao et
355 al. 2019) or decreased soil water availability (Bertolino et al. 2019). In addition to guard cell length and
356 stomatal density, foliar or wood $\delta^{18}O$ signature has been widely used as an indicator for g_s and shifts
357 therein. This $\delta^{13}C$ and $\delta^{18}O$ dual isotope approach was established to relate changes in iWUE to changes
358 in either g_s or photosynthesis (Scheidegger et al. 2000). As there is no detectable trend in leaf $\delta^{18}O$ in our
359 study, this would suggest that the actual g_s did not vary over time, and that the iWUE response is mainly
360 driven by reduced photosynthesis. However, recent work has cautioned against the use of $\delta^{18}O$ as a
361 proxy for g_s in areas where relative humidity is high (Farquhar et al. 2007, Roden and Siegwolf 2012).
362 Indeed, after simulating the $\delta^{18}O$ with our tool (Appendix 1) and with the parameterization we used for
363 our site in central Africa, $\delta^{18}O$ appears to be insensitive to g_s (Figure S2). As a result, the interpretation of
364 these and other $\delta^{18}O$ data as a proxy for g_s from the tropics should be done with great care.

365
366 For photosynthesis, there is no direct proxy that integrates the photosynthetic activity of the leaves.
367 Instead, we looked at foliar nutrients that have been widely related to photosynthetic capacity (Evans
368 1989, Kattge et al. 2009, Walker et al. 2014, Tränkner et al. 2018). As such, the foliar N, P, and Mg show a
369 slight increase over time. Along with the decreasing stomatal density, this increase in leaf nutrients
370 seems to suggest a rather strong adaptation of central African trees to environmental change: less
371 potential water loss via a ca. 30% decrease in stomatal density and an apparent higher potential
372 photosynthetic capacity via a 5-20% increase in leaf nutrients.

373
374 The combination of a decreasing stomatal density and apparent upregulation in photosynthetic capacity
375 would result in an expected increasing iWUE, but yet iWUE decreases over time. This paradoxical
376 response challenges our current paradigms of tropical rainforest responses to environmental change,
377 and points to additional variables acting on the forest other than only CO_2 fertilization. Recent reports on
378 the increase of boreal summer dry season length in the Congo basin (Jiang et al. 2019), in combination
379 with a decline of the greenness of the Congo tropical forest in the last decade (Zhou et al. 2014),
380 highlight a biome-specific change that might be linked to this unique response to a regional change.
381 Indeed, long-term drying since the 1950s in central Africa (Dai 2013), along with longer dry seasons,
382 higher temperatures, and increases in photosynthetic active radiation (Zhou et al. 2014) separates the

383 Congo basin forest from the Amazon forest, which is subjected to episodic short-term droughts (Phillips
384 et al. 2009, Saatchi et al. 2013). Such long-term drying trend and increasing temperatures would surely
385 impact the forest evapotranspiration via an increase in the vapor pressure deficit (VPD). Drought
386 experiments have shown that plants maximize transpiration in that case, provided the available soil
387 water levels are high enough. Although it is assumed that the sensitivity of photosynthesis to VPD is
388 likely weaker than the sensitivity of g_s to VPD, it is still substantial. As a result, the overall relationship
389 between $iWUE$ and VPD is likely hyperbolic and $iWUE$ can decline as VPD continues to rise (Zhang et al.
390 2019, Grossiord et al. 2020). More importantly, if this drying trend is accompanied by an air temperature
391 increase, than this ensemble might shift local conditions to the extent that the temperature optimum for
392 photosynthesis is exceeded, resulting in a depression of net photosynthesis (Lin et al. 2012, Aubry-Kientz
393 et al. 2019, Huang et al. 2019). This holds especially for tropical forests, which already operate near a
394 high temperature optimum, above which canopy photosynthesis may decrease with moderate air
395 temperature warming (Huang et al. 2019). Indeed, it has been shown that the plasticity for thermal
396 acclimation at the leaf level in tropical trees is limited, with potentially strong negative effects on leaf
397 photosynthesis (Cheesman and Winter 2013, Dusenge and Way 2017, Slot and Winter 2017). We
398 confirmed these climatic trends using the CRUNCEP data (Viovy 2018) for the grid cell of our study site,
399 and looked at trends in temperature, VPD, relative humidity and precipitation, and additionally
400 maximum temperature using the Berkeley data (Rohde et al. 2013). Although we have to keep in mind
401 that these data are based on interpolation and re-analyses, our site seems to have experienced an
402 increasing temperature, with maximum temperatures exceeding the 30°C since 1970 (Figure S7), which
403 approximately corresponds to optimal temperature for photosynthesis in the tropics (Huang et al. 2019).
404 Additionally, precipitation has slightly decreased and VPD increased over that same period. All together,
405 these environmental changes could be responsible for a simultaneous increase in water deficit and water
406 demand in this biome, combined with a reduction of net photosynthesis. The maximum temperature
407 increase might push central African tropical forests over the physiological optimum temperature for
408 photosynthesis, but with a high VPD and hence high transpiration. If this is at the basis of the decreasing
409 $iWUE$ trend, then this is likely of importance for other tropical forest biomes as well, as temperatures are
410 projected to increase across the tropics. However, more experimental work is needed to test this
411 observation in detail. Additionally, some authors have cautioned against the use of a linear, simplified
412 relationship between $\delta^{13}C$ and $iWUE$, because $iWUE$ might be influenced by other factors such as
413 mesophyll conductance (Seibt et al. 2008). Indeed, a systematic change over time in mesophyll
414 conductance could underlie any $\delta^{13}C$ trend and more research is needed to assess such effects. We
415 acknowledge the importance of such biases but also note the clear practical limitation to assess
416 mesophyll conductance in tree-ring or herbarium studies. Altogether, we can only conclude from our
417 data that net photosynthesis in our study site cannot be upregulated proportionally to changes in water-

418 use, which has resulted in higher concentrations of CO₂ in the stomatal cavity and subsequently in a
419 decreasing iWUE.

420
421 **Ruling out sampling bias.** Our variance decomposition of the present-day sample set from Yangambi and
422 Luki (Figure 4) showed that up to 35% of the variation in leaf N, leaf P, and leaf Mg can be attributed to
423 the canopy level of sampling. Therefore, we have to consider that a sampling effect is potentially
424 contributing to the observed leaf nutrient trends. Indeed, the variance decomposition indicated that
425 higher, sunlit leaves, have structurally higher nutrient contents (Figure 4). However, the older herbarium
426 specimens supposedly comprised sunlit leaves, while the 2013-collected samples were sampled with
427 climbers, and were thus a mixture of sun and shade leaves. This means that the increasing nutrient
428 content is potentially underestimated and the real increase in nutrient content might be larger than the
429 trends detected in this study (Figure 2). For stomata, on the other hand, there seems to be a decrease in
430 density from samples in the lower canopy (Figure 4) but not on the order of magnitude of the temporal
431 decrease that was noted in the herbarium specimens (Figure 2.; -22 mm⁻² versus -84 mm⁻², respectively).
432 Additionally, previous work has shown high variability in both whole-plant iWUE and the
433 photosynthetic/stomatal responsiveness to increasing CO₂ across tropical tree species (Cernusak et al.
434 2007, Hasper et al. 2017). Nevertheless, the general trend across 23 common tree species that cover a
435 wide range in the trait space is a decreasing iWUE.

436
437 One additional challenge in using δ¹³C as a proxy for environmental information stored in plants is the
438 influence of tree height on δ¹³C (Brienen et al. 2017). Although there is very little structural variance in
439 δ¹³C associated with canopy level (Figure 4), we have used the variance dataset (2% relative positive
440 effect of upper canopy sampling, 1% relative negative effect of sampling lower canopy) to test if an
441 extreme sampling bias could have changed our trend in iWUE. If we hence assume that samples from
442 1938 were overestimated by 2%, and samples in 2013 underestimated with 1% relative to their mean,
443 then we still see a clear and significant decreasing iWUE (Figure S6). This implies that a decreasing iWUE
444 trend at our site cannot be caused by a sampling bias at the canopy level.

445
446 **No proof of progressive nutrient limitation** To our knowledge, only one study has reported a decrease in
447 iWUE, which took place in a subtropical P-limited forest (Huang et al. 2016). The latter study links the
448 decreasing iWUE to the combination of P limitation, aggravated by high on-site N deposition. This
449 aggravated P limitation was apparent from both the increasing leaf N:P ratio and decreasing leaf P. Like
450 this site in subtropical China, our central African study site is also P-limited and subjected to high N
451 deposition (Bauters et al. 2018, 2019). However, contrary to the site in south China, no shifts in N:P ratio
452 could be detected, while the leaf P in the leaves seems to have been increasing. Indeed, shifts in Huang

453 et al. in N:P ratio, along with a decreasing P content shows trends that are very similar to aggravated P
454 limitation that was noted along a primary succession (Izquierdo et al. 2013). In contrast, the lack of a
455 shift in C:N or N:P ratios in our data seems to suggest that there is no progressive N or P limitation in
456 central Africa. Additionally, the overall leaf P increases over time, despite the fact that lowland tropical
457 trees are assumed to be P limited (Vitousek et al. 2010) since they grow on strongly weathered and P-
458 poor oxisols (Walker and Syers 1976). However, the way this species-level P limitation manifests as a
459 community-wide response is still debated (Turner et al. 2018, Fleischer et al. 2019). In any case, we find
460 no direct proof of N or P becoming increasingly limiting or increasingly constraining the C balance of the
461 forest at our study site. This is contrary to what we would expect from theory and model simulations
462 (Bonan 2008b, Wieder et al. 2015), and suggests that an increasing P limitation is either simply not
463 reflected in the canopy stoichiometry, or is not yet occurring. In the latter case, external nutrient inputs
464 could alleviate an increasing nutrient limitation. Biomass burning in the savanna borders on the African
465 continent seems to give rise to an extraordinarily high N deposition on central African forests (Bauters et
466 al. 2018), with seemingly no direct export that matches the N input (Bauters et al. 2019). Whether this
467 also causes high organic P or airborne particle-bound P deposition on these forests, potentially
468 alleviating an aggravated N or P limitation, is currently unknown.

469
470 **Implications for the Congo Basin's C balance.** The implication of the observed physiological leaf-level
471 response, i.e. the overall interactive effect of CO₂ fertilization and other environmental change factors on
472 the whole-ecosystem C balance, is widely debated. Model simulations and empirical results from Free Air
473 CO₂ Enrichment (FACE) experiments suggest an increase in net primary productivity, constrained by
474 nutrient bioavailability (Norby et al. 2005, 2010, 2017), while tree-ring research from the tropics suggests
475 that a change in iWUE does not lead to a long-term increased biomass accrual or growth stimulation
476 (Nock et al. 2011, van der Sleen et al. 2014). In temperate regions, an increasing iWUE coincided with
477 decreasing growth induced by warming (Penuelas et al. 2008). Unfortunately, FACE experiments are
478 currently lacking in the tropics, so direct evidence for the CO₂ fertilization effect on tropical productivity
479 is still missing (Norby and Zak 2011, Cernusak et al. 2013). Additionally, long-term adaptation of plant
480 physiology or a delayed soil nutrient constraint might also lead to an overestimation of the CO₂
481 fertilization effects on net primary productivity from FACE experiments (Norby and Zak 2011, Peñuelas et
482 al. 2011, Reich and Hobbie 2013). Indeed, ecosystem-level interpretations which are based on shifts in
483 leaf-level iWUE alone are not trivial. At the very least, however, the decreasing iWUE raises questions on
484 the implications for the Congo basin forest's C balance at large scale. Further on-ground monitoring with
485 repeated censuses and with more advanced ecosystem-level monitoring tools (e.g. eddy covariance
486 towers) are needed to address this knowledge gap, given the importance of this biome for the global C
487 cycle.

488

489 **Conclusion**

490 Tropical forests are important in our global understanding of the changing C balance, but empirical
491 evidence of responses to environmental changes is sparse. The Congo basin's forest seems to show a
492 unique response, exhibiting decreasing iWUE since 1938, with a downregulation of stomatal density and
493 without a clear upregulation of photosynthetic capacity. Via an additional study on the variability of the
494 measured variables in canopies, we can safely exclude that the iWUE trend shown in this study is not
495 driven by sampling bias. This observed response challenges our current understanding of CO₂ fertilization
496 on tropical terrestrial ecosystems. For now, we can only conclude that environmental factors other than
497 increasing CO₂, e.g. increasing maximum temperature, likely overprints the expected iWUE response of
498 central African trees. Still, more work is needed to mechanistically quantify these effects . The overall
499 impact of this decreasing iWUE on the whole ecosystem C balance is unknown, but without doubt
500 critical. Finally, we did not find proof of the progressive nutrient limitation hypothesis, exhibited by the
501 lack of shifts in leaf nutrient stoichiometry since 1938 documented in this study.

502

503 **Supplementary information**

504 **Figure S1.** The response in leaf $\delta^{18}\text{O}$ to changes in stomatal conductance, as a function of the relative
505 humidity, as simulated by the excel tool in Appendix 1, based on the model of Lorrey et al. (2016).

506 **Figure S2.** Bulk leaf $\delta^{13}\text{C}$ vs leaf cellulose $\delta^{13}\text{C}$.

507 **Figure S3.** The evolution of 1) leaf carbon stable isotope composition and intrinsic water-use efficiency
508 (iWUE); 2) leaf nitrogen (N), leaf phosphorus (P) and leaf magnesium (Mg), as nutrient proxies related to
509 photosynthesis, and 3) stomatal density (SD) and guard cell length (GCL) and the stable oxygen isotope
510 signature over the last century in central African tropical forest, with separation of nitrogen fixers and
511 non-fixers.

512 **Figure S4.** Shifts in C:N, N:P and C:P stoichiometry since 1938 for central African trees, with separation of
513 nitrogen fixers and non-fixers.

514 **Figure S5.** Examples of stomata microscope images of herbarium specimens of nine tropical tree species

515 **Figure S6.** Trends in leaf carbon stable isotopic composition and intrinsic water-use efficiency with a
516 correction for an hypothetical (and maximum) sampling bias

517 **Figure S7.** The trends in air temperature, precipitation, relative humidity, vapor pressure deficit and
518 maximum temperature from 1935 to 2010 for our study location.

519 **Table S1.** Species and herbarium specimens that were included in the analyses for the different time
520 periods.

521 **Table S2.** Species-specific thresholds and information retrieval standard measures (precision, recall and
522 F-score) for a validation set of three microphotographs per species ($N = 18$).

523 **Table S3.** General site characteristics

524

525 **Appendix**

526 **A1.** An excel-tool to simulate the $\delta^{18}\text{O}$ signature in leaves as a response to changes in stomatal
527 conductance, relative humidity, temperature, wind speed, source water $\delta^{18}\text{O}$ and water vapor $\delta^{18}\text{O}$,
528 based on earlier models by Barbour et al. (2004) and Lorrey et al. (2016). Explanation on how to use the
529 tool is provided in the Excel file itself. It also includes an interactive sensitivity analysis.

530

531 **Data Accessibility**

532 Data supporting the results in this paper are available via the Supplementary Information or archived in
533 the Ghent University institutional repository, and available upon request with the corresponding author.

534

535 **Acknowledgments**

536 We want to thank the collectors of the herbarium specimens, that have greatly advanced our insights in
537 central African tree ecology. We also want to thank Rolf Siegwolf and David Ellsworth for valuable
538 comments and insights on parts of this study. Both M.B. and F.M. are funded by the Research
539 Foundation – Flanders (FWO-Vlaanderen) through a postdoctoral fellowship. S.M. is funded by the
540 COBECORE BELSPO-project (Brain.be – code: BR/175/A3/COBECORE). H.D.D. is supported via an
541 European Research Council Starting Grant 637643 (TREECLIMBERS), and the analyses in this study are
542 funded through both the COBECORE project and an FWO KAN project grant 1507818N.

543 **Literature cited**

544 Adams, M. A., Turnbull, T. L., Sprent, J. I., & Buchmann, N. (2016). Legumes are different: Leaf
545 nitrogen, photosynthesis, and water use efficiency. *Proceedings of the National Academy of*
546 *Sciences of the United States of America*, *113*(15), 4098–4103.

547 <https://doi.org/10.1073/pnas.1523936113>

548
549 Aubry-Kientz, M., Rossi, V., Cornu, G., Wagner, F., & Hérault, B. (2019). Temperature rising
550 would slow down tropical forest dynamic in the Guiana Shield. *Scientific Reports*, *9*(1), 1–8.
551 <https://doi.org/10.1038/s41598-019-46597-8>

552
553 Baker, T. R., Phillips, O. L., Malhi, Y., Almeida, S., Arroyo, L., Di Fiore, A., ... Missouri, B.
554 De. (2004). Variation in wood density determines spatial patterns in Amazonian forest
555 biomass. *Global Change Biology*, *10*, 545–562. [https://doi.org/10.1111/j.1529-](https://doi.org/10.1111/j.1529-8817.2003.00751.x)
556 [8817.2003.00751.x](https://doi.org/10.1111/j.1529-8817.2003.00751.x)

557
558
559 Ballantyne, A. P., Alden, C. B., Miller, J. B., Trans, P. P., & White, J. W. C. (2012). Increase in
560 observed net carbon dioxide uptake by land and oceans during the past 50 years. *Nature*,
561 *488*(7409), 70–73. <https://doi.org/10.1038/nature11299>

562
563 Barbour, M. M., Roden, J. S., Farquhar, G. D., & Ehleringer, J. R. (2004). Expressing leaf water
564 and cellulose oxygen isotope ratios as enrichment above source water reveals evidence of a
565 Péclet effect. *Oecologia*, *138*(3), 426–435. <https://doi.org/10.1007/s00442-003-1449-3>

566
567 Bates, D., Sarkar, D., Bates, M. D., & Matrix, L. (2007). The lme4 Package. *October*, *2*(1), 1–6.
568 <https://doi.org/10.18637/jss.v067.i01>

569
570 Bauters, M., Drake, T. W., Verbeeck, H., Bodé, S., Hervé-Fernandez, P., Zito, P., ... Boeckx, P.
571 (2018). High fire-derived nitrogen deposition on central African forests. *Proceedings of the*
572 *National Academy of Sciences*, *115*(3), 549–554. <https://doi.org/10.1073/pnas.1714597115>

573
574 Bauters, M., Verbeeck, H., Rütting, T., Barthel, M., Bazirake Mujinya, B., Bamba, F., ...
575 Boeckx, P. (2019). Contrasting nitrogen fluxes in African tropical forests of the Congo
576 Basin. *Ecological Monographs*, *89*(1), e01342. <https://doi.org/10.1002/ecm.1342>

577
578 Beer, C., Reichstein, M., Tomelleri, E., Ciais, P., Jung, M., Carvalhais, N., ... Papale, D. (2010).
579 Terrestrial Gross Carbon dioxide uptake: Global distribution and covariation with Climate.
580 *Science*, 329(August), 834–839.
581
582 Bertolino, L. T., Caine, R. S., & Gray, J. E. (2019). Impact of stomatal density and morphology
583 on water-use efficiency in a changing world. *Frontiers in Plant Science*, 10.
584 <https://doi.org/10.3389/fpls.2019.00225>
585
586 Bonal, D., Ponton, S., Le Thiec, D., Richard, B., Ningre, N., Hérault, B., ... Guehl, J. M. (2011).
587 Leaf functional response to increasing atmospheric CO₂ concentrations over the last
588 century in two northern Amazonian tree species: A historical $\delta^{13}\text{C}$ and $\delta^{18}\text{O}$ approach
589 using herbarium samples. *Plant, Cell and Environment*, 34(8), 1332–1344.
590 <https://doi.org/10.1111/j.1365-3040.2011.02333.x>
591
592 Bonan, G. B. (2008). Forests and climate change: forcings, feedbacks, and the climate benefits of
593 forests. *Science (New York, N.Y.)*, 320, 1444–1449. <https://doi.org/10.1126/science.1155121>
594
595 Bonan, G. B. (2008). Carbon cycle: Fertilizing change. *Nature Geoscience*, 1, 645–646.
596 <https://doi.org/10.1038/ngeo328>
597
598 Brendel, O., Iannetta, P. P. M., & Stewart, D. (2000). A Rapid and Simple Method to Isolate Pure
599 Alpha- cellulose. *Phytochemical Analysis*, 11, 7–10.
600
601 Brien, R. J. W., Gloor, E., Clerici, S., Newton, R., Arppe, L., Boom, A., ... Timonen, M.
602 (2017). Tree height strongly affects estimates of water-use efficiency responses to climate
603 and CO₂ using isotopes. *Nature Communications*, 8(1), 1–10.
604 <https://doi.org/10.1038/s41467-017-00225-z>
605
606 Brien, R. J. W. R. J. W. R. J. W. R. J. W., Wanek, W., & Hietz, P. (2010). Stable carbon
607 isotopes in tree rings indicate improved water use efficiency and drought responses of a
608 tropical dry forest tree species. *Trees*, 25(1), 103–113. [https://doi.org/10.1007/s00468-010-](https://doi.org/10.1007/s00468-010-0474-1)
609 0474-1
610

- 611 Bürkner, P. C. (2017). brms: An R package for Bayesian multilevel models using Stan. *Journal*
612 *of Statistical Software*. <https://doi.org/10.18637/jss.v080.i01>
613
- 614 Cernusak, L. A., Aranda, J., Marshall, J. D., & Winter, K. (2007). Large variation in whole-plant
615 water-use efficiency among tropical tree species. *New Phytologist*, *173*(2), 294–305.
616 <https://doi.org/10.1111/j.1469-8137.2006.01913.x>
617
- 618 Cernusak, L. A., Winter, K., Dalling, J. W., Holtum, o. A. M., Jaramillo, C., Körner, C., ...
619 Wright, S. J. (2013). Tropical forest responses to increasing atmospheric CO₂ : Current
620 knowledge and opportunities for future research. *Functional Plant Biology*, *40*(6), 531–551.
621 <https://doi.org/10.1071/FP12309>
622
- 623 Cheesman, A. W., & Winter, K. (2013). Growth response and acclimation of CO₂ exchange
624 characteristics to elevated temperatures in tropical tree seedlings, *64*(12), 3817–3828.
625 <https://doi.org/10.1093/jxb/ert211>
626
- 627 Clark, D. B., Clark, D. a., & Oberbauer, S. F. (2010). Annual wood production in a tropical rain
628 forest in NE Costa Rica linked to climatic variation but not to increasing CO₂. *Global*
629 *Change Biology*, *16*(2), 747–759. <https://doi.org/10.1111/j.1365-2486.2009.02004.x>
630
- 631 Craine, J. M., Elmore, A. J., Wang, L., Aranibar, J., Bauters, M., Boeckx, P., ... Zmudczyńska-
632 Skarbek, K. (2018). Isotopic evidence for oligotrophication of terrestrial ecosystems. *Nature*
633 *Ecology & Evolution* *2018 2:11*, *2*(11), 1735. <https://doi.org/10.1038/s41559-018-0694-0>
634
- 635 Dai, A. (2013). Increasing drought under global warming in observations and models. *Nature*
636 *Climate Change*, *3*(1), 52–58. <https://doi.org/10.1038/nclimate1633>
637
- 638 Deng, J., Dong, W., Socher, R., Li, L., Li, K., & Fei-fei, L. (2009). ImageNet : A Large-Scale
639 Hierarchical Image Database. *2009 IEEE Conference on Computer Vision and Pattern*
640 *Recognition*, 248–255. <https://doi.org/10.1109/CVPR.2009.5206848>
641
- 642 Doetterl, S., Kearsley, E., Bauters, M., Hufkens, K., Lisingo, J., Baert, G., ... Boeckx, P. (2015).
643 Aboveground vs. Belowground Carbon Stocks in African Tropical Lowland Rainforest:

644 Drivers and Implications. *Plos One*, 10(11), e0143209.
645 <https://doi.org/10.1371/journal.pone.0143209>
646
647 Dusenge, M. E., & Way, D. A. (2017). Warming puts the squeeze on photosynthesis – lessons
648 from tropical trees. *Journal of Experimental Botany*, (2013), 0–4.
649
650 Evans, J. R. (1989). Photosynthesis and nitrogen relationships in leaves of C3 plants. *Oecologia*,
651 78(1), 9–19. <https://doi.org/10.1007/BF00377192>
652
653 Farquhar, G. D., Cernusak, L. A., & Barnes, B. (2007). Heavy water fractionation during
654 transpiration. *Plant Physiology*, 143(1), 11–18. <https://doi.org/10.1104/pp.106.093278>
655
656 Farquhar, G. D., Leary, M. H. O. and Berry, J. A. (1982). On the relationship between carbon isotope
657 discrimination and the intercellular carbon dioxide concentration in leaves. *Australian journal of*
658 *plant physiology*, 9:121–37.
659
660 Farquhar, G. D., & Richards, R. A. (1984). Isotopic composition of plant carbon correlates with
661 water-use efficiency of wheat genotypes. *Australian Journal of Plant Physiology*, 11(6),
662 539–552. <https://doi.org/10.1071/PP9840539>
663
664 Feeley, K. J., Wright, S. J., Supardi, M. N. N., Kassim, A. R., & Davies, S. J. (2007).
665 Decelerating growth in tropical forest trees. *Ecology Letters*, 10(6), 461–469.
666 <https://doi.org/10.1111/j.1461-0248.2007.01033.x>
667
668 Fernandez-Martinez, M., Vicca, S., Janssens, I. a., Sardans, J., Luyssaert, S., Campioli, M., ...
669 Reichstein, M. (2014). Nutrient availability as the key regulator of global forest carbon
670 balance. *Nature Climate Change*, 4(June), 471–476.
671 <https://doi.org/10.1038/NCLIMATE2177>
672
673 Fleischer, K., Rammig, A., De Kauwe, M. G., Walker, A. P., Domingues, T. F., Fuchslueger, L.,
674 ... Lapola, D. M. (2019). Amazon forest response to CO2 fertilization dependent on plant
675 phosphorus acquisition. *Nature Geoscience*, 12, 736–741. [https://doi.org/10.1038/s41561-](https://doi.org/10.1038/s41561-019-0404-9)
676 [019-0404-9](https://doi.org/10.1038/s41561-019-0404-9)
677

- 678 Friedli, H., Löttscher, H., Oeschger, H., Siegenthaler, U., & Stauffer, B. (1986). Ice core record of
679 the $^{13}\text{C}/^{12}\text{C}$ ratio of atmospheric CO_2 in the past two centuries. *Nature*, *324*, 698–699.
680 <https://doi.org/10.1038/320129a0>
681
- 682 Gibson, L., Lee, T. M., Koh, L. P., Brook, B. W., Gardner, T. A., Barlow, J., ... Sodhi, N. S.
683 (2011). Primary forests are irreplaceable for sustaining tropical biodiversity. *Nature*,
684 *478*(7369), 378–381. *Journal*. <https://doi.org/10.1038/nature10425>
685
- 686 Groenendijk, P., van der Sleen, P., & Vlam, M. (2015). No evidence for consistent long-term
687 growth stimulation of 13 tropical tree species : results from tree-ring analysis. *Global*
688 *Change Biology*, *3762–3776*. <https://doi.org/10.1111/gcb.12955>
689
- 690 Grossiord, C., Buckley, T. N., Cernusak, L. A., Novick, K. A., Poulter, B., Siegwolf, R. T. W., ...
691 McDowell, N. G. (2020). Plant responses to rising vapor pressure deficit. *New Phytologist*,
692 *Early View*. <https://doi.org/10.1111/nph.16485>
693
- 694 Hasper, T. B., Dusenge, M. E., Breuer, F., Uwizeye, F. K., Wallin, G., & Uddling, J. (2017).
695 Stomatal CO_2 responsiveness and photosynthetic capacity of tropical woody species in
696 relation to taxonomy and functional traits. *Oecologia*, *184*(1), 43–57.
697 <https://doi.org/10.1007/s00442-017-3829-0>
698
- 699 Hietz, P., Turner, B. L., Wanek, W., Richter, A., Nock, C. a., & Wright, S. J. (2011). Long-term
700 change in the nitrogen cycle of tropical forests. *Science*, *334*(November), 664–666.
701 <https://doi.org/10.1126/science.1211979>
702
- 703 Hietz, P., Wanek, W., & Dünisch, O. (2005). Long-term trends in cellulose $\delta^{13}\text{C}$ and water-use
704 efficiency of tropical *Cedrela* and *Swietenia* from Brazil. *Tree Physiology*, *25*(6), 745–752.
705
- 706 Huang, Z., Liu, B., Davis, M., Sardans, J., Peñuelas, J., & Billings, S. (2016). Long-term nitrogen
707 deposition linked to reduced water use efficiency in forests with low phosphorus
708 availability. *New Phytologist*, *210*(2), 431–442. <https://doi.org/10.1111/nph.13785>
709

- 710 Huang, M., Piao, S., Ciais, P., Peñuelas, J., Wang, X., Keenan, T. F., ... Janssens, I. A. (2019).
711 Air temperature optima of vegetation productivity across global biomes. *Nature Ecology*
712 *and Evolution*, 3(5), 772–779. <https://doi.org/10.1038/s41559-019-0838-x>
713
- 714 Izquierdo, J. E., Houlton, B. Z., & van Huysen, T. L. (2013). Evidence for progressive
715 phosphorus limitation over long-term ecosystem development: Examination of a
716 biogeochemical paradigm. *Plant and Soil*, 367(1–2), 135–147.
717 <https://doi.org/10.1007/s11104-013-1683-3>
718
- 719 Jiang, Y., Zhou, L., Tucker, C. J., Raghavendra, A., Hua, W., Liu, Y. Y., & Joiner, J. (2019).
720 Widespread increase of boreal summer dry season length over the Congo rainforest. *Nature*
721 *Climate Change*, 4, 1–8. <https://doi.org/10.1038/s41558-019-0512-y>
722
- 723 Jiao, X. C., Song, X. M., Zhang, D. L., Du, Q. J., & Li, J. M. (2019). Coordination between vapor
724 pressure deficit and CO₂ on the regulation of photosynthesis and productivity in greenhouse
725 tomato production. *Scientific Reports*, 9(1), 1–10. [https://doi.org/10.1038/s41598-019-](https://doi.org/10.1038/s41598-019-45232-w)
726 [45232-w](https://doi.org/10.1038/s41598-019-45232-w)
727
- 728 Jonard, M., Fürst, A., Verstraeten, A., Thimonier, A., Timmermann, V., Potočić, N., ... Rautio,
729 P. (2015). Tree mineral nutrition is deteriorating in Europe. *Global Change Biology*, 21(1),
730 418–430. <https://doi.org/10.1111/gcb.12657>
731
- 732 Kattge, J., Knorr, W., Raddatz, T., & Wirth, C. (2009). Quantifying photosynthetic capacity and
733 its relationship to leaf nitrogen content for global-scale terrestrial biosphere models. *Global*
734 *Change Biology*, 15(4), 976–991. <https://doi.org/10.1111/j.1365-2486.2008.01744.x>
735
- 736 Keeling, C. D., Bacastow, R. B. B., Carter, A. F. F., Piper, S. C. C., Whorf, T. P. T. P., Heimann,
737 M., ... Roeloffzen, H. (1989). A three-dimensional model of atmospheric CO₂ transport
738 based on observed winds: 1. Analysis of observational data. *Geophysical Monograph*, 55, 1–
739 6. <https://doi.org/10.1029/gm055p0165>
740
- 741 Keeling, R. F., Graven, H. D., Welp, L. R., Resplandy, L., Bi, J., Piper, S. C., ... Meijer, H. A. J.
742 (2017). Atmospheric evidence for a global secular increase in carbon isotopic discrimination

743 of land photosynthesis. *Proceedings of the National Academy of Sciences*, 114(39), 10361–
744 10366. <https://doi.org/10.1073/pnas.1619240114>
745
746 Keenan, T. F., Hollinger, D. Y., Bohrer, G., Dragoni, D., Munger, J. W., Schmid, H. P., &
747 Richardson, A. D. (2013). Increase in forest water-use efficiency as atmospheric carbon
748 dioxide concentrations rise. *Nature*, 499(7458), 324–327.
749 <https://doi.org/10.1038/nature12291>
750
751 Kingma, D. P., & Ba, J. L. (2015). Adam: A method for stochastic optimization. *ArXiv Preprint*
752 *ArXiv:1412.6980*.
753
754 Kuznetsova, A., Brockhoff, P. B., & Christensen, R. H. B. (2014). lmerTest: Tests for random
755 and fixed effects for linear mixed effect models (lmer objects of lme4 package). *R Package*
756 *Version*. <https://doi.org/http://CRAN.R-project.org/package=lmerTest>
757
758 Lavergne, A., Graven, H., De Kauwe, M. G., Keenan, T. F., Medlyn, B. E., & Prentice, I. C.
759 (2019). Observed and modelled historical trends in the water-use efficiency of plants and
760 ecosystems. *Global Change Biology*, 25(7), 2242–2257. <https://doi.org/10.1111/gcb.14634>
761
762 Lavergne, A., Voelker, S., Csank, A., Graven, H., de Boer, H. J., Daux, V., ... Prentice, I. C.
763 (2020). Historical changes in the stomatal limitation of photosynthesis: empirical support for
764 an optimality principle. *New Phytologist*, 225(6), 2484–2497.
765 <https://doi.org/10.1111/nph.16314>
766
767 Lewis, S. L., Lopez-Gonzalez, G., Sonké, B., Affum-Baffoe, K., Baker, T. R., Ojo, L. O., ...
768 Wöll, H. (2009). Increasing carbon storage in intact African tropical forests. *Nature*,
769 457(7232), 1003–1006. <https://doi.org/10.1038/nature07771>
770
771 Li, Y., Niu, S., & Yu, G. (2016). Aggravated phosphorus limitation on biomass production under
772 increasing N addition: A meta-analysis. *Global Change Biology*, 22(2), 934–943.
773 <https://doi.org/10.1111/gcb.13125>
774

- 775 Lin, Y. S., Medlyn, B. E., & Ellsworth, D. S. (2012). Temperature responses of leaf net
776 photosynthesis: The role of component processes. *Tree Physiology*, 32(2), 219–231.
777 <https://doi.org/10.1093/treephys/tpr141>
778
- 779 Lorrey, A. M., Brookman, T. H., Evans, M. N., Fauchereau, N. C., Macinnis-ng, C., Barbour, M.
780 M., ... Schrag, D. P. (2016). Stable oxygen isotope signatures of early season wood in New
781 Zealand kauri (*Agathis australis*) tree rings : Prospects for palaeoclimate reconstruction.
782 *Dendrochronologia*, 40, 1–14.
783
- 784 McLauchlan, K. K., Ferguson, C. J., Wilson, I. E., Ocheltree, T. W., & Craine, J. M. (2010).
785 Thirteen decades of foliar isotopes indicate declining nitrogen availability in central North
786 American grasslands. *New Phytologist*, 187(4), 1135–1145. [https://doi.org/10.1111/j.1469-
787 8137.2010.03322.x](https://doi.org/10.1111/j.1469-8137.2010.03322.x)
788
- 789 McLauchlan, K. K., Gerhart, L. M., Battles, J. J., Craine, J. M., Elmore, A. J., Higuera, P. E., ...
790 Perakis, S. S. (2017). Centennial-scale reductions in nitrogen availability in temperate
791 forests of the United States. *Scientific Reports*, 7(1), 1–7. [https://doi.org/10.1038/s41598-
792 017-08170-z](https://doi.org/10.1038/s41598-017-08170-z)
793
- 794 Meeus, S., Van den Bulcke, J. and Wyffels, F. Under review . From leaf to label: a robust automated
795 workflow for stomata detection. *Methods in Ecology and Evolution*.
796
- 797 Meineke, E. K., Davis, C. C., & Davies, T. J. (2018). The unrealized potential of herbaria for
798 global change biology. *Ecological Monographs*, 88(4), 505–525.
799 <https://doi.org/10.1002/ecm.1307>
800
- 801 Nock, C. A., Baker, P. J., Wanek, W., Leis, A., Grabner, M., Bunyavejchewin, S., & Hietz, P.
802 (2011). Long-term increases in intrinsic water-use efficiency do not lead to increased stem
803 growth in a tropical monsoon forest in western Thailand. *Global Change Biology*, 17(2),
804 1049–1063. <https://doi.org/10.1111/j.1365-2486.2010.02222.x>
805
- 806 Norby, R. J., Delucia, E. H., Gielen, B., Calfapietra, C., Giardina, C. P., King, J. S., ... Oren, R.
807 (2005). Forest response to elevated CO₂ is conserved across a broad range of productivity.

808 *Proceedings of the National Academy of Sciences of the United States of America*, 102(50),
809 18052–18056. <https://doi.org/10.1073/pnas.0509478102>
810

811 Norby, R. J., De Kauwe, M. G., Walker, A. P., Werner, C., Zaehle, S., & Zak, D. R. (2017).
812 Comment on “Mycorrhizal association as a primary control of the CO₂ fertilization effect.”
813 *Science*, 355(6323), 358b. <https://doi.org/10.1126/science.aai7976>
814

815 Norby, R. J., Warren, J. M., Iversen, C. M., Medlyn, B. E., & McMurtrie, R. E. (2010). CO₂
816 enhancement of forest productivity constrained by limited nitrogen availability. *Proceedings*
817 *of the National Academy of Sciences of the United States of America*, 107(45), 19368–
818 19373. <https://doi.org/10.1073/pnas.1006463107>
819

820 Norby, R. J., & Zak, D. R. (2011). Ecological Lessons from Free-Air CO₂ Enrichment (FACE)
821 Experiments. *Annual Review of Ecology, Evolution, and Systematics*, 42(1), 181–203.
822 <https://doi.org/10.1146/annurev-ecolsys-102209-144647>
823

824 O’Leary, M. H. (1981). Carbon isotope fractionation in plants. *Phytochemistry*, 20(4), 553–567.
825 [https://doi.org/10.1016/0031-9422\(81\)85134-5](https://doi.org/10.1016/0031-9422(81)85134-5)
826

827 Pan, Y., Birdsey, R. a, Fang, J., Houghton, R., Kauppi, P. E., Kurz, W. a, ... Hayes, D. (2011). A
828 large and persistent carbon sink in the world’s forests. *Science*, 333(6045), 988–993.
829 <https://doi.org/10.1126/science.1201609>
830

831 Peñuelas, J., Canadell, J. G., & Ogaya, R. (2011). Increased water-use efficiency during the 20th
832 century did not translate into enhanced tree growth. *Global Ecology and Biogeography*,
833 20(4), 597–608. <https://doi.org/10.1111/j.1466-8238.2010.00608.x>
834

835 Penuelas, J., Hant, J. M., Ogaya, R., & Jump, A. S. (2008). Twentieth century changes of tree-
836 ring d 13 C at the southern range-edge of *Fagus sylvatica* : increasing water-use efficiency
837 does not avoid the growth decline induced by warming at low altitudes. *Global Change*
838 *Biology*, 14, 1076–1088. <https://doi.org/10.1111/j.1365-2486.2008.01563.x>
839

840 Peñuelas, J., Poulter, B., Sardans, J., Ciais, P., van der Velde, M., Bopp, L., ... Janssens, I. a.
841 (2013). Human-induced nitrogen-phosphorus imbalances alter natural and managed

842 ecosystems across the globe. *Nature Communications*, 4, 2934.
843 <https://doi.org/10.1038/ncomms3934>
844
845 Phillips, O. L. (1998). Changes in the Carbon Balance of Tropical Forests: Evidence from Long-
846 Term Plots. *Science*, 282(5388), 439–442. <https://doi.org/10.1126/science.282.5388.439>
847
848 Phillips, O. L., Aragão, L. E. O. C., Lewis, S. L., Fisher, J. B., Lloyd, J., López-gonzález, G., ...
849 Salamão, R. (2009). Drought Sensitivity of the Amazon Rainforest. *Science*, 323(March),
850 1344–1347.
851
852 R Development Core Team. (2018). R: A language and environment for statistical computing.
853 Vienna, Austria, <http://www.r-project.org>. <https://doi.org/10.1007/978-3-540-74686-7>
854
855 Rohde, R., Muller, R., Jacobsen, R., Perlmutter, S., & Mosher, S. (2013). Berkeley Earth
856 Temperature Averaging Process. *Geoinformatics & Geostatistics: An Overview*.
857 <https://doi.org/10.4172/2327-4581.1000103>
858
859 Reich, P. B., & Hobbie, S. E. (2013). Decade-long soil nitrogen constraint on the CO2
860 fertilization of plant biomass. *Nature Climate Change*, 3(3), 278–282.
861 <https://doi.org/10.1038/nclimate1694>
862
863 Roden, J., & Siegwolf, R. (2012). Is the dual-isotope conceptual model fully operational? *Tree*
864 *Physiology*, 32(10), 1179–1182. <https://doi.org/10.1093/treephys/tps099>
865
866 Ryan, J., Estefan, G., & Rashid, A. (2001). *Soil and Plant Analysis Laboratory Manual. Second*
867 *Edition*. Aleppo, Syria, Syria: ICARDA.
868
869
870 Saatchi, S., Asefi-Najafabady, S., Malhi, Y., Aragão, L. E. O. C., Anderson, L. O., Myneni, R.
871 B., & Nemani, R. (2013). Persistent effects of a severe drought on Amazonian forest
872 canopy. *Proceedings of the National Academy of Sciences of the United States of America*,
873 110(2), 565–570. <https://doi.org/10.1073/pnas.1204651110>
874

- 875 Scheidegger, Y., Saurer, M., Bahn, M., Siegwolf, R., Scheidegger, Y., Saurer, M., ... Siegwolf,
876 R. (2000). Linking stable oxygen and carbon isotopes with stomatal conductance and
877 photosynthetic capacity : a conceptual model. *Oecologia*, 350–357.
878 <https://doi.org/10.1007/s004420000466>
879
- 880 Schimel, D., Pavlick, R., Fisher, J. B., Asner, G. P., Saatchi, S., Townsend, P., ... Cox, P. (2015).
881 Observing terrestrial ecosystems and the carbon cycle from space. *Global Change Biology*,
882 21(5), 1762–1776. <https://doi.org/10.1111/gcb.12822>
883
- 884 Schindelin, J., Arganda-carreras, I., Frise, E., Kaynig, V., Schmid, B., Tinevez, J., ... Hartenstein,
885 V. (2012). Fiji : an open-source platform for biological-image analysis. *Nature Methods*,
886 9(7), 676–682. <https://doi.org/10.1038/nmeth.2019>
887
- 888 Schubert, B. A., & Jahren, A. H. (2018). Incorporating the effects of photorespiration into
889 terrestrial paleoclimate reconstruction. *Earth-Science Reviews*, 177(November 2017), 637–
890 642. <https://doi.org/10.1016/j.earscirev.2017.12.008>
891
- 892 Seibt, U., Rajabi, A., Griffiths, H., & Berry, J. A. (2008). Carbon isotopes and water use
893 efficiency: Sense and sensitivity. *Oecologia*, 155(3), 441–454.
894 <https://doi.org/10.1007/s00442-007-0932-7>
895
- 896 Silva, L. C. R., Anand, M., Oliveira, J. M., & Pillar, V. D. (2009). Past century changes in
897 *Araucaria angustifolia* (Bertol.) Kuntze water use efficiency and growth in forest and
898 grassland ecosystems of southern Brazil: Implications for forest expansion. *Global Change*
899 *Biology*, 15(10), 2387–2396. <https://doi.org/10.1111/j.1365-2486.2009.01859.x>
900
- 901 Simonyan, K., & Zisserman, A. (2014). Very deep convolutional networks for large-scale image
902 recognition. *ArXiv Preprint ArXiv:1409.1556*.
903
- 904 Slot, M., & Winter, K. (2017). Photosynthetic acclimation to warming in tropical forest tree
905 seedlings. *Journal of Experimental Botany*, 68(9), 2275–2284.
906 <https://doi.org/10.1093/jxb/erx071>
907

908 Sokolov, A. P., Kicklighter, D. W., Melillo, J. M., Felzer, B. S., Schlosser, C. A., & Cronin, T.
909 W. (2008). Consequences of considering carbon-nitrogen interactions on the feedbacks
910 between climate and the terrestrial carbon cycle. *Journal of Climate*, 21(15), 3776–3796.
911 <https://doi.org/10.1175/2008JCLI2038.1>
912
913 Steffen, W., Richardson, K., Rockstrom, J., Cornell, S. E., Fetzer, I., Bennett, E. M., ... Sorlin, S.
914 (2015). Planetary boundaries: Guiding human development on a changing planet. *Science*,
915 347(6223), 1259855–1259855. <https://doi.org/10.1126/science.1259855>
916
917 Tränkner, M., Tavakol, E., & Jákli, B. (2018). Functioning of potassium and magnesium in
918 photosynthesis, photosynthate translocation and photoprotection. *Physiologia Plantarum*,
919 163(3), 414–431. <https://doi.org/10.1111/ppl.12747>
920
921 Turner, B. L., Brenes-Arguedas, T., & Condit, R. (2018). Pervasive phosphorus limitation of tree
922 species but not communities in tropical forests. *Nature*, 555(7696), 367–370.
923 <https://doi.org/10.1038/nature25789>
924
925
926 Van Der Sleen, P., Groenendijk, P., Vlam, M., Anten, N. P. R., Boom, A., Bongers, F., ...
927 Zuidema, P. A. (2015). No growth stimulation of tropical trees by 150 years of CO₂
928 fertilization but water-use efficiency increased. *Nature Geoscience*, 8(1), 24–28.
929 <https://doi.org/10.1038/ngeo2313>
930
931 Van Ranst, E., G. Baert, M. Ngongo, and P. Mafuka. 2010. Carte pédologique de Yangambi, planchette 2:
932 Yangambi, échelle 1:50.000. UGent, Hogent, UNILU, UNIKIN.
933
934 Viovy, N. 2018. CRUNCEP Version 7 - Atmospheric Forcing Data for the Community Land Model. Research
935 Data Archive at the National Center for Atmospheric Research, Computational and Information
936 Systems Laboratory. <https://doi.org/10.5065/PZ8F-F017>. Accessed† 31-01-2020.
937
938 Vitousek, P. M., Porder, S., Houlton, B. Z., & Chadwick, O. A. (2010). Terrestrial phosphorus
939 limitation : mechanisms , implications , and nitrogen – phosphorus interactions. *Ecological*
940 *Applications*, 20(1), 5–15. <https://doi.org/10.1890/08-0127.1>
941

- 942 Walker, A. P., Beckerman, A. P., Gu, L., Kattge, J., Cernusak, L. A., Domingues, T. F., ...
943 Woodward, F. I. (2014). The relationship of leaf photosynthetic traits - V_{cmax} and J_{max} - to
944 leaf nitrogen, leaf phosphorus, and specific leaf area: A meta-analysis and modeling study.
945 *Ecology and Evolution*, 4(16), 3218–3235. <https://doi.org/10.1002/ece3.1173>
946
- 947 Walker, T. W., & Syers, J. K. (1976). The fate of phosphorus during pedogenesis. *Geoderma*, 15,
948 1–19.
949
- 950 Wang, M., Chen, Y., Wu, X., & Bai, Y. (2018). Forest-Type-Dependent Water Use Efficiency
951 Trends Across the Northern Hemisphere. *Geophysical Research Letters*, 45(16), 8283–8293.
952 <https://doi.org/10.1029/2018GL079093>
953
- 954 Wieder, W. R., Cleveland, C. C., Smith, W. K., & Todd-Brown, K. (2015). Future productivity
955 and carbon storage limited by terrestrial nutrient availability. *Nature Geoscience*, 8, 441–
956 444. <https://doi.org/10.1038/ngeo2413>
957
- 958 Xu, Z., Jiang, Y., Jia, B., & Zhou, G. (2016). Elevated- CO_2 response of stomata and its
959 dependence on environmental factors. *Frontiers in Plant Science*, 7(MAY2016), 1–15.
960 <https://doi.org/10.3389/fpls.2016.00657>
961
- 962 Zhang, Q., Ficklin, D. L., Manzoni, S., Wang, L., Way, D., Phillips, R. P., & Novick, K. A.
963 (2019). Response of ecosystem intrinsic water use efficiency and gross primary productivity
964 to rising vapor pressure deficit. *Environmental Research Letters*, 14(7).
965 <https://doi.org/10.1088/1748-9326/ab2603>
966
- 967 Zhou, L., Tian, Y., Myneni, R. B., Ciais, P., Saatchi, S., Liu, Y. Y., ... Hwang, T. (2014).
968 Widespread decline of Congo rainforest greenness in the past decade. *Nature*, 508(7498),
969 86–90. <https://doi.org/10.1038/nature13265>